Analyst

PAPER

View Article Online
View Journal | View Issue

Cite this: *Analyst*, 2025, **150**, 5411

Development of one-step magnetic assay for the detection of fentanyl

Fabiana Grillo, [a] Elena Piletska, [a] Ewa Moczko, [a] César Cáceres [b] and Sergey Piletsky *[a]

This study introduces a novel one-step magnetic immunoassay (mMINA) designed for effective and sensitive detection of fentanyl, a potent synthetic opioid. The proposed method offers several advantages over the standard ELISA protocol, notably a substantial reduction in procedural steps from sample application to analysis. Simplicity directly translates into saved time, lowered measurement costs, minimized potential for errors, and enhanced user-friendliness and precision. The assay utilizes 96-well magnetic microplates for solid-phase separation, fluorescently labeled anti-fentanyl antibodies, and fentanyl-functionalized iron oxide nanoparticles as competing probes. Upon co-incubation, free fentanyl in the sample competes with nanoparticle-bound fentanyl for limited antibody binding, resulting in an inversely proportional fluorescence signal. The method demonstrated high specificity and sensitivity, with a limit of detection (LoD) of 1.562 nM in blood plasma, and showed high selectivity with structurally similar opioids such as morphine, heroin, or cocaine. It maintained performance in complex biological matrices, underscoring its robustness and reproducibility. Importantly, the modular platform design, based on commercially available antibodies, allows adaptation to other small-molecule targets. This flexibility, combined with operational simplicity and low cost, positions the mMINA assay as a practical tool for rapid drug screening in clinical, forensic, and field-based settings.

Received 30th March 2025,
Accepted 2nd November 2025

DOI: 10.1039/d5an00361j

rsc.li/analyst

1. Introduction

Significant reports such as the United Nations Office on Drugs and Crime (UNODC) report or the European drug report highlight serious trend of increasing mortality rates due to drug overdoses.[1–3] This complex issue is influenced by various factors including drug availability, accessibility to treatment, socioeconomic factors, and the potency of drugs available on the market. Particularly alarming is the widespread presence of fentanyl, a highly potent synthetic opioid, which poses a significant challenge in cases of drug misuse and overdose.[4,5] Even a small amount of fentanyl might lead to rapid excess and death.[6–8] While fentanyl is a medication approved by the Food and Drug Administration for analgesic and anaesthetic purposes, its illicitly manufactured variants are frequently found in a variety of street drugs, including heroin, cocaine, methamphetamine, and counterfeit prescription medications. Fentanyl is 50 times more powerful than heroin and 100 times-than morphine.[9–11] The prevalence of fentanyl contamination in drugs and the subsequent unintentional consumption remain major concerns for public health and law enforcement agencies worldwide. Hence, there is need for rapid, accessible, and low-budget detection systems for drugs of abuse (DOA) with particular attention on detection of fentanyl.

Nowadays, several methods are available on the market to identify the presence of this compound in various media. The major one involves immunoassay testing.[12–15] It utilizes commercially available kits employing antibodies that specifically bind to fentanyl mmolecules, producing a measurable signal. Immunoassay tests are rapid and commonly used for preliminary screening in settings like drug rehabilitation centers, emergency rooms, and law enforcement.[13,16–18] While immunoassay testing offers several advantages, it also has some drawbacks such as cross-reactivity with structurally similar compounds, leading to false-positive results.[19,20] Substances like tramadol, diphenhydramine, and certain antidepressants can potentially interfere with the test, producing inaccurate results. Immunoassays may not detect low concentrations of fentanyl, particularly in samples with high levels of interference from other substances. They are time consuming and costly. Alternatively, mass spectrometry GC-MS, LC-MS and high-performance liquid chromatography (HPLC) can be used.[21–23] These are standard powerful techniques that can identify and quantify the molecular composition of substances with high precision and accuracy. Unfortunately, the cost of

[a]*School of Chemistry, University of Leicester, Leicester, LE1 7RH, UK. E-mail: sp523@leicester.ac.uk*
[b]*Facultad de Farmacia, Escuela de Química y Farmacia, Universidad de Valparaíso, Gran Bretaña 1093, Valparaíso, Chile*

the equipment, its maintaining, and operating is high. This can be a barrier for smaller laboratories or facilities with limited budgets. Additionally, it requires specialized training and expertise to operate and interpret results. Sample preparation can be labour-intensive and analyzing data can be complex, and time-consuming. HPLC analysis can also be susceptible to interference from the sample matrix, especially in complex biological specimens such as blood or urine.[24,25] The other options might be nuclear magnetic resonance (NMR) spectroscopy, surface-enhanced Raman spectroscopy (SERS) or ion mobility spectrometry (IMS), but in practice they are all complicated and require advance training and high-cost recourses.[26–28] Therefore there is a need in developing advanced assay formats that require minimum handling and capable of producing accurate measurements in short time.

Herein, we present novel method of the detection of fentanyl, using one-step assay performed in magnetic microtiter plates and based on magnetic, fentanyl iron oxide nanoparticles (f_IO_NPs) and the commercially available anti-fentanyl antibodies. Magnetic microplate-based platforms were prepared as described previously.[29] They have emerged as a promising alternative to traditional solid-phase immunoassay formats due to their ease of handling, automation compatibility, and capacity for high-throughput analysis. Unlike conventional well plates or microbeads, magnetic plates allow spatially confined, uniform immobilization of reagents while enabling efficient magnetic separation without the need for centrifugation or filtration steps. These systems have been applied in diverse biosensing contexts, including detection of pathogens, hormones, and small-molecule drugs, with notable reductions in assay time and reagent consumption. Their integration with fluorescence-based readout further enhances sensitivity and simplifies signal acquisition. Given these advantages, magnetic microplates are particularly well-suited for rapid, low-complexity competitive immunoassays such as the one presented in this study. Recent studies have demonstrated their utility in point-of-care and portable testing formats, making them attractive for deployment in clinical and field-based settings. Schematic illustration of new methodology is presented in Fig. 1.

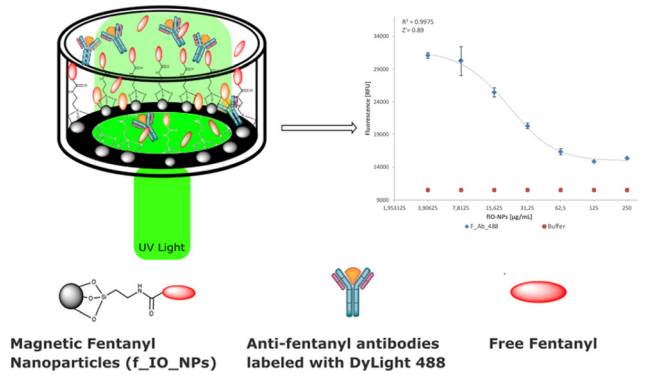

Fig. 1 Schematic representation of the magnetic microplate-based immunoassay (mMINA) for fentanyl detection. Left: The assay mixture: free fentanyl (analyte), fluorescently labeled anti-fentanyl antibodies (f_Ab_488), and fentanyl-functionalized iron oxide nanoparticles (f_IO_NPs). Incubation in a competitive binding format, where free fentanyl competes with surface-bound fentanyl for binding to f_Ab_488. Right: Fluorescent intensity of unbound f_Ab_488 in the supernatant following incubation and magnetic separation, measured at λ_{ex} = 493 nm, λ_{em} = 518 nm. The signal is inversely proportional to the concentration of fentanyl in the sample.

2. Experimental section

2.1. Materials

Anti-fentanyl antibodies (mouse monoclonal) were purchased from Creative Diagnostics. DyLight 488, fentanyl, iron(II) sulfate heptahydrate ($FeSO_4{\cdot}7H_2O$, 99%), iron(III) chloride hexahydrate ($FeCl_3{\cdot}6H_2O$, 99%), *N*-hydroxysuccinimide (NHS), *N*-(3-dimethylaminopropyl)-*N*′-ethylcarbodiimide hydrochloride (EDC, ≥98%), sodium chloride (NaCl, 99%), phosphate buffered saline (PBS), sulfuric acid (H_2SO_4), acetone, ethanol, acetic acid, dimethylformamide (DMF), 3-aminopropyltriethoxysilane (APTES), [3-(2-aminoethylamino)propyl] trimethoxysilane (AEAPTMS), and lyophilized human blood plasma (S2257-5ML) were purchased from Sigma-Aldrich. Milli-Q water (Millipore) was used throughout. All chemicals and solvents were of analytical or HPLC grade and were used without further purification. Polystyrene microplates were purchased from Thermo Scientific, UK. Amicon® Ultra-4 centrifugal filter units (3 kDa cutoff) were obtained from Merck.

2.2. Methods

Synthesis of iron oxide nanoparticles. $FeSO_4{\cdot}7H_2O$ (6 g, 21.6 mmol) and $FeCl_3{\cdot}6H_2O$ (7 g, 25.9 mmol) were dissolved in 200 mL of degassed Milli-Q water in 500 mL round-bottom flask under N_2. The solution was heated to 85 °C with vigorous stirring (100 rpm). Once the temperature stabilized, an aqueous solution of 25% ammonia (25% w/w, 15 mL) was then quickly added in one portion, leading to a change of colour from orange to black due to the precipitation of the magnetic nanoparticles (indicating nanoparticles formation). The rection mixture was stirred at 85 °C for an additional 30 min and then allowed to cool down to ambient temperature. Afterwards, the black precipitate was magnetically separated and washed sequentially with deionized water (3 × 50 mL), 0.2 M NaCl solution (1 × 50 mL) and acetone (2 × 50 mL). Nanoparticles were dried under N_2 and stored at 4 °C.

Silanisation of iron oxide nanoparticles (IO_NP). A 50 mL solution containing 5% v/v water in ethanol was prepared, and pH was adjusted to 4.5–5.5 using acetic acid. The silane coupling agents, APTES and AEAPTMS, were dissolved in aqueous solution, mixed 1 : 1 molar ratio and left for 5 min at ambient temperature. After flashing with N_2, 200 mg of dried IO_NPs were added to the solution and sonicated in water bath (40 kHz) for 4 h. The silanized particles were washed with 5% ethanol in deionized water (5 × 250 mL), dried under N_2, and cured in an oven at 110 °C for 1 h. IO_NPs were stored in a vacuum desiccator overnight.

Fentanyl immobilisation on iron oxide nanoparticles (IO_NP). Carboxyl-fentanyl was dissolved in 1 mL ethanol. EDC (5.7 mg mL^{-1}) and NHS (3.4 mg mL^{-1}) were dissolved in 1 mL PBS and mixed with fentanyl solution. The reaction was left to occur for 7 min. In a meanwhile, 200 mg of IO_NP were suspended in 8 mL of PBS (10 mM, pH 7.4) and sonicated for 5 min. After that the solution of carboxyl-fentanyl EDC/NHS was added to the silanized IO_NP suspension. The reaction mixture was left under continuous shaking for 4 h, ambient temperature. The modified particles were washed 10 times with methanol using magnetic separation to remove unreacted reagents and stored at 4 °C.

Antibody fluorescent labelling with DyLight 488. Anti-fentanyl antibodies were first reconstructed in PBS (0.01 M, pH 7.4) at a concentration of 1 mg mL^{-1}, as per manufacturer instructions. Labelling of antibodies was performed by dissolving 50 μg of DyLight 488 NHS-ester (M_w: 1011 g mol^{-1}) in 50 μL of DMF and adding dropwise to 250 μL of antibody solution under gentle stirring. The reaction proceeded for 4 h in the dark at ambient temperature. Excess dye and unreacted components were removed by centrifugal filtration (10 cycles, 2 mL, 0.01 M PBS per cycle) using Amicon® Ultra-4, 3 kDa filters. Filtration was performed for 10 min at 4 °C and 3600 rpm. The absence of residual fluorescence in the last wash was confirmed *via* fluorescence measurement. Aliquots ware stored at 4 °C (short term, ≤2 weeks) or −20 °C (long term).

Final competitive assay procedure. The assay was performed in a total volume of 100 μL. A binding mixture was prepared containing 10 μg mL^{-1} of DyLight 488-labeled anti-fentanyl antibody (f_Ab_488), 31.25 μg mL^{-1} fentanyl-IO_NPs, and varying concentrations of free fentanyl (6.25–200 nM) in PBS (10 mM, pH 7.4). The mixture was added to wells of a 96-microtitre plate and incubated in ambient temperature for 45 minutes in the dark on a plate shaker at 300 rpm to allow competitive binding. Following incubation, the magnetic beads were separated using a magnetic insert and the supernatants (containing unbound fluorescent antibody) were carefully transferred to a black 96-well flat-bottom plate. Fluorescence intensity was measured with excitation at 485 nm and emission at 518 nm. Each sample and standard was measured in triplicate. Control wells included antibody-only (no nanoparticles), nanoparticle-only (no antibody), and blank PBS to correct for background fluorescence. For blood plasma assays, the protocol was identical except fentanyl standards were spiked into 10% (v/v) human blood plasma. Signal suppression and matrix effects were accounted for by subtracting background fluorescence from blood plasma-only control wells.

3. Results and discussion

3.1. Optimization of antibody–nanoparticle binding

The first stage in the assay development was to investigate the dynamics and efficiency of the binding between the fluorescently labelled anti-fentanyl antibodies (f_Ab_488) and varying amounts of fentanyl-functionalized iron oxide nanoparticles (f_IO_NPs). It was done by using fixed concentration of f_Ab_488 (10 μg mL^{-1}) incubated with increasing concentrations of f_IO_NPs (3.9–2000 μg mL^{-1}). The concentration of antibody was selected according to the literature, as it is the standard concentration used in immunoassays. The fluorescence intensity of the supernatant was measured to evaluate the extent of antibody binding. As shown in Fig. 2, fluorescence intensity decreased with increasing nanoparticle concentration, indicating successful binding of f_Ab_488 to f_IO_NPs. Saturation was achieved at concentrations ≥125 μg mL^{-1}, suggesting that nearly all antibodies were bound. A half-maximal binding point (50% binding) was observed at approximately 22.5 μg mL^{-1} of f_IO_NPs (R^2 = 0.9975), which was selected as the working concentration for subsequent competitive binding assays.

As can be seen in Fig. 2, at f_IO_NPs concentration equal or major to 125 μg mL^{-1}, no change in fluorescence is observed, indicating that all of the f_Ab_488 in solution is already bound to f_IO_NPs. At 7.8 and 62.5 μg mL^{-1} the fluorescence was directly proportional to the concentration of magnetic NPs, with 50% of binding reached at a concentration of f_IO_NPs of 22.5 μg mL^{-1} (R^2 of 0.9975), which was selected as the working concentration for subsequent competitive binding assays.

A competitive assay format was employed to assess the assay's ability to quantify free fentanyl. A fixed concentration of f_Ab_488 (10 μg mL^{-1}) and f_IO_NPs (31.25 μg mL^{-1}) was incubated for 45 min with varying concentrations of free fentanyl (1.28–4000 nM). As the concentration of free fentanyl increased, fluorescence intensity in the supernatant increased due to decreased antibody binding to nanoparticle-bound fentanyl.

The assay exhibited a sigmoidal response curve, with a defined linear detection range between 1.5 and 400 nM (see Fig. 3). Saturation occurred at concentrations below 6.4 nM

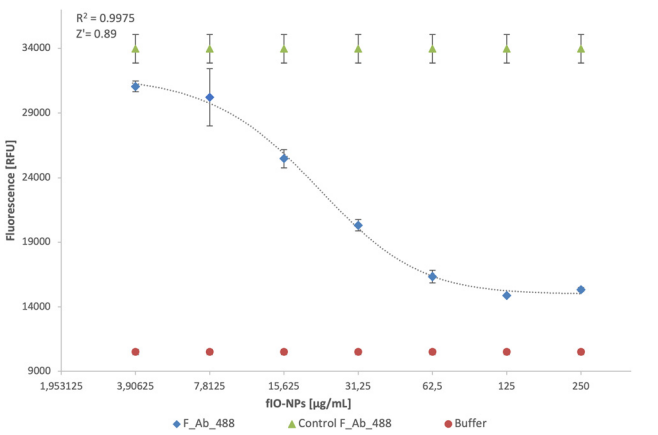

Fig. 2 Binding experiment between fluorescently labeled anti-fentanyl antibody (f_Ab_488) and fentanyl-functionalized iron oxide nanoparticles (f_IO_NPs). Fluorescence intensity is plotted as a function of increasing concentrations of f_IO_NPs (3.9–2000.0 μg mL^{-1}) in the presence of a fixed concentration of f_Ab_488 (10 μg mL^{-1}, blue curve). The green curve represents the control with f_Ab_488 in the absence of nanoparticles. The red curve corresponds to buffer-only background.

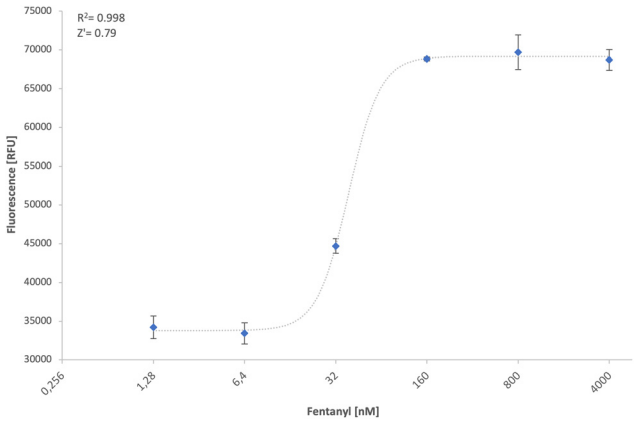

Fig. 3 Competitive binding experiment for fentanyl quantification using fluorescently labeled anti-fentanyl antibody (f_Ab_488) and fentanyl-functionalized iron oxide nanoparticles (f_IO_NPs). The assay was performed using a fixed concentration of f_Ab_488 (10 μg mL^{-1}) and f_IO_NPs (31.25 μg mL^{-1}), while varying the concentration of free fentanyl (1.28–4000.00 nM). This figure illustrates the qualitative trend of fluorescence response across increasing fentanyl concentrations. The *x*-axis represents log scale, log [C].

and above 160 nM, suggesting a reliable dynamic range for quantification of fentanyl in relevant concentrations for clinical and forensic applications. Fig. 3, similarly to Fig. 4, presents qualitative fluorescence responses across a range of analyte concentrations. These data were intended to demonstrate assay responsiveness rather than to define a quantitative working range. Accordingly, we describe these results in terms of relative signal changes rather than attempting curve fitting or establishing a definitive dynamic range.

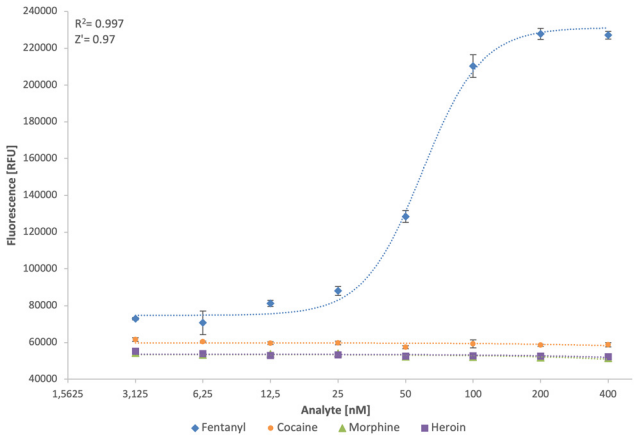

Fig. 4 Selectivity assay experiment to evaluate assay specificity toward fentanyl. The assay was conducted using fluorescently labeled anti-fentanyl antibody (f_Ab_488, 10 μg mL^{-1}) and fentanyl-functionalized iron oxide nanoparticles (f_IO_NPs, 31.25 μg mL^{-1}). Free analytes—fentanyl (blue), cocaine (orange), morphine (green), and heroin (purple)—were added at concentrations ranging from 1.56 to 800.00 nM. Each trace represents incubation with a single analyte only (fentanyl, cocaine, morphine, or heroin). Buffer control (red) was included for background comparison. The *x*-axis represents log scale, log [C].

The optimised concentrations were used to assess the specificity of the assay. Therefore, a selectivity study was performed using f_IO_NPs incubated with f_Ab_488, free fentanyl and structurally related drugs, including cocaine, morphine and heroin.

These drugs were tested at the same concentration as fentanyl under identical conditions. The results (see Fig. 4 and 5) demonstrated that although morphine, heroin, and cocaine produced fluorescence signals above the buffer baseline, these responses were not concentration-dependent and remained

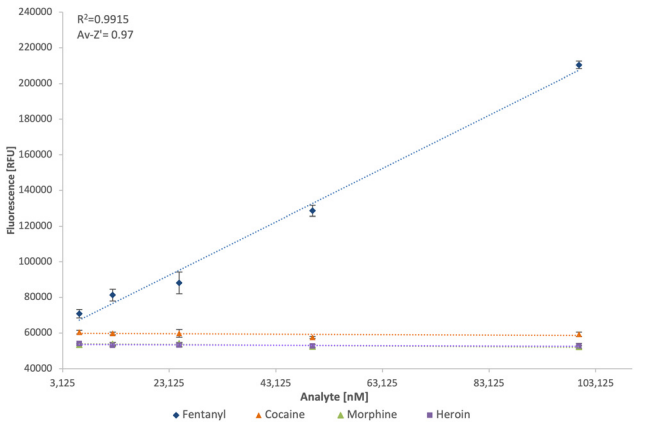

Fig. 5 Linear range of the competition assay for fentanyl detection and its selectivity with structurally related compounds. The assay was performed using fluorescently labeled anti-fentanyl antibody (f_Ab_488, 10 μg mL^{-1}) and fentanyl-functionalized iron oxide nanoparticles (f_IO_NPs, 31.25 μg mL^{-1}). Fluorescence intensity was measured in the presence of increasing concentrations (1.56–800.00 nM) of free fentanyl (blue), cocaine (orange), morphine (green), and heroin (purple), with buffer (red) serving as the negative control. While the strongest linearity was observed in the 40–100 nM region, lower concentrations were included in the fit to illustrate the total working range of the assay. Each trace represents incubation with a single analyte only (fentanyl, cocaine, morphine, or heroin).

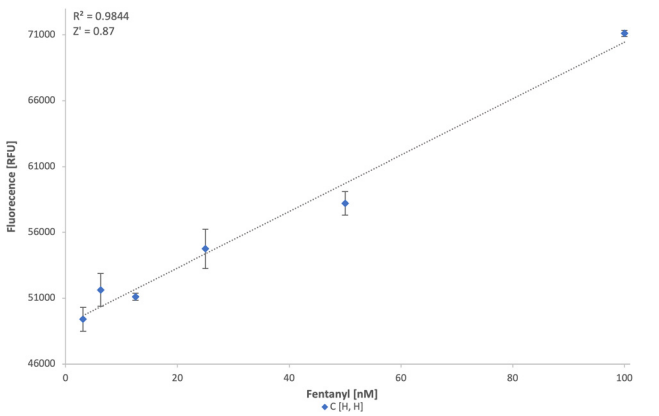

Fig. 6 High-sensitivity competition assay for fentanyl detection. The assay was conducted using fluorescently labeled anti-fentanyl antibody (f_Ab_488, 10 μg mL^{-1}) and fentanyl-functionalized iron oxide nanoparticles (f_IO_NPs, 0.25 mg mL^{-1}). Increasing concentrations of free fentanyl (0.78–400.00 nM) were added to assess the assay's sensitivity.

Table 1 Comparison between the developed mMINA with commercially available ELISAs from Creative Diagnostics® and Neogen®

	Assay technology	Washing steps	Incubations steps	Total assay incubation time	Detection limit in blood plasma
Magnetic assay developed	Competition, fluorescence	None	1	45 min	0.525 ng mL^{-1}
Fentanyl assay CD®	Competition, enzyme conjugation, absorbance	2 × 3 times	3	75 min	—
Fentanyl assay Neogen®	Competition, enzyme conjugation, absorbance	2 × 3 times	3	75 min	0.25 ng mL^{-1}

consistently below the established limit of detection (LoD) for fentanyl. As such, they are considered non-specific background and do not compromise the assay's ability to selectively detect fentanyl.

This confirms that the assay is very selective for fentanyl, with toward commonly encountered interfering substances. Additionally, the regression line in Fig. 5 spans the full 2–100 nM range, the most consistent linearity was observed between 40 nM and 100 nM. The inclusion of lower concentrations in the fit reflects the assay's response across its full tested range, though slight deviations from linearity may occur at low signal levels.

The robustness of the assay was further evaluated using spiked human blood plasma samples. Free fentanyl was added to 10% (v/v) human blood plasma in concentrations ranging from 0.78 to 400 nM. Despite the presence of biological matrix components, the assay maintained a clear concentration-dependent response (see Fig. 6), with a limit of detection (LoD) of 1.562 nM (equivalent to 0.525 ng mL^{-1}). The assay retained a linear response in the range of 6.25 to 200 nM, demonstrating good matrix tolerance and suitability for real-world biological samples. Although the assay demonstrated clear signal discrimination across tested concentrations, additional studies are needed to define its full quantitative dynamic range.

The performance of the developed magnetic assay was compared with commercially available ELISA kits from Creative Diagnostics® and Neogen® (see Table 1). While both commercial kits rely on enzyme-conjugated antibodies and require multiple washing steps and longer incubation times (75 minutes total), the mMINA method operates with a single incubation step, no washing, and a total assay time of 45 minutes. Although the LoD of the magnetic assay (0.525 ng mL^{-1} in blood plasma) is slightly higher than that of Neogen® (0.25 ng mL^{-1} in blood plasma), the time and labor savings, combined with the reduced risk of error, present significant practical advantages for fentanyl detection.

4. Conclusions

In this study, we developed a one-step competitive magnetic immunoassay (mMINA) targeting fentanyl. By integrating magnetic microplates, fluorescently labeled anti-fentanyl antibodies, and fentanyl-functionalized iron oxide nanoparticles, the assay enables rapid, accurate, and specific detection within a simplified and user-friendly format.

This platform achieved a limit of detection (LoD) of 1.562 nM in blood plasma and demonstrated excellent specificity, showing good selectivity with structurally similar opioids such as morphine, heroin or cocaine. This novel magnetic assay offers significant advantages over conventional methods, such as ELISA or mass spectrometry, by minimizing handling steps, reducing assay time to 45 minutes, and eliminating the need for multiple washing and incubation steps. Its streamlined workflow lowers the risk of procedural errors, reduces operational costs, and enhances usability in diverse settings, including forensic, medical, and public health applications. Importantly, the assay also maintained performance in complex matrices, confirming its robustness and anti-interference capability. The platform's modular design, based on commercially available antibodies, allows it to be readily adapted for detection of other analytes. This flexibility, combined with cost-effectiveness and operational simplicity, positions the assay as a valuable tool for rapid drug screening and monitoring.

In conclusion, the proposed mMINA format represents a significant step forward in fentanyl detection technologies, offering a practical, scalable, and efficient alternative to traditional methods. Additionally, in rapid and high-throughput drug detection. Its combination of sensitivity, specificity, and anti-interference performance supports its potential for real-world application and routine practice.

Conflicts of interest

There are no conflicts to declare.

Data availability

The data that support the findings of this study are available from the corresponding author, Prof. Sergey Piletsky, upon request.

References

1 UNODC, *World Drug Report*, 2021.
2 P. O. o. t. E. Union, *European Drug Report 2023: trends and developments*, 2023.
3 N. Wilson, M. Kariisa, P. Seth, H. Smith and N. L. Davis, *Morb. Mortal. Wkly. Rep.*, 2020, **69**, 290–297.

4 S. L. Hedrick, D. Luo, S. Kaska, K. K. Niloy, K. Jackson, R. Sarma, J. Horn, C. Baynard, M. Leggas, E. R. Butelman, M. J. Kreek and T. E. Prisinzano, *J. Biomed. Sci.*, 2021, **28**, 18.
5 S. M. Cibulsky, T. Wille, R. Funk, D. Sokolowski, C. Gagnon, M. Lafontaine, C. Brevett, R. Jabbour, J. Cox, D. R. Russell, D. A. Jett, J. D. Thomas and L. S. Nelson, *Front. Public Health*, 2023, **11**, 1–9.
6 K. Walter, *JAMA, J. Am. Med. Assoc.*, 2023, **329**, 184–184.
7 P. T. Bremer, E. L. Burke, A. C. Barrett and R. I. Desai, *Nat. Commun.*, 2023, **14**, 7700.
8 S. Crunkhorn, *Nat. Rev. Drug Discovery*, 2024, **23**, 107.
9 D. E. A. Drug and Chemical Evaluation Section. Office of Diversion Control, 2023, https://www.deadiversion.usdoj.gov/drug_chem_info/fentanyl.pdf, accessed on 06 November 2025.
10 R. E. Wharton, J. S. Casbohm, R. Hoffmaster, B. N. Brewer, M. G. Finn and R. C. Johnson, *J. Anal. Toxicol.*, 2021, **45**(2), 111–116.
11 B. Zhang, X. Hou, C. Zhen and A. X. Wang, *Biosensors*, 2021, **11**, 370.
12 P. T. Bremer, E. L. Burke, A. C. Barrett and R. I. Desai, *Nat. Commun.*, 2023, **14**, 7700.
13 C. Norman, V. Marland, C. McKenzie, H. Ménard and N. N. Daéid, *Int. J. Drug Policy*, 2023, **118**, 104102.
14 S. Crunkhorn, *Nat. Rev. Drug Discovery*, 2024, **23**, 107–107.
15 R. E. Wharton, J. Casbohm, R. Hoffmaster, B. N. Brewer, M. G. Finn and R. C. Johnson, *J. Anal. Toxicol.*, 2021, **45**, 111–116.
16 J. C. Halifax, L. Lim, D. Ciccarone and K. L. Lynch, *Harm Reduct. J.*, 2024, **21**, 14.
17 S. E. Rodriguez-Cruz, *J. Forensic Sci.*, 2023, **68**, 1555–1569.
18 G. R. Williams, M. Akala and C. E. Wolf, *Clin. Biochem.*, 2023, **113**, 45–51.
19 J. C. Halifax, L. Lim, D. Ciccarone and K. L. Lynch, *Harm Reduct. J.*, 2024, **21**, 14.
20 S. E. Rodriguez-Cruz, *J. Forensic Sci.*, 2023, **68**, 1555–1569.
21 G. R. Williams, M. Akala and C. E. Wolf, *Clin. Biochem.*, 2023, **113**, 45–51.
22 C. Liu, T. Li, Y. Han, Z. Hua, W. Jia and Z. Qian, *Drug Test. Anal.*, 2018, **10**, 774–780.
23 H. E. McKeown, T. J. Rook, J. R. Pearson and O. A. H. Jones, *Forensic Chem.*, 2023, **33**, 100476.
24 F. P. Busardò, J. Carlier, R. Giorgetti, A. Tagliabracci, R. Pacifici, M. Gottardi and S. Pichini, *Front. Chem.*, 2019, **7**, 184.
25 N. H. Huynh, N. Tyrefors, L. Ekman and M. Johansson, *J. Pharm. Biomed. Anal.*, 2005, **37**, 1095–1100.
26 B. X. Zhang, X. W. Hou, C. Zhen and A. X. Wang, *Biosensors*, 2021, **11**, 370.
27 H. E. McKeown, T. J. Rook, J. R. Pearson and O. A. H. Jones, *Forensic Chem.*, 2020, **21**, 100285.
28 C. M. Liu, T. Li, Y. Han, Z. D. Hua, W. Jia and Z. H. Qian, *Drug Test. Anal.*, 2018, **10**, 774–780.
29 E. V. Piletska, S. S. Piletsky, A. Guerreiro, K. Karim, M. J. Whitcombe and S. A. Piletsky, *J. Chin. Adv. Mater. Soc.*, 2014, **2**, 118–129.